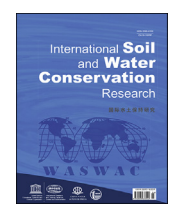


Contents lists available at ScienceDirect

# International Soil and Water Conservation Research

journal homepage: www.elsevier.com/locate/iswcr



Original Research Article

# Feedback mechanism between gully landforms and sediment trapping efficiency in a check dam



Jiangang Chen <sup>a, b, c</sup>, Xi'an Wang <sup>a, b</sup>, Huayong Chen <sup>a, b, c</sup>, Wanyu Zhao <sup>a, b, c</sup>, Chenyuan Wang <sup>a, b</sup>, Xiaoqing Chen <sup>a, b, c</sup>,

- <sup>a</sup> State Key Laboratory of Natural Hazards and Engineering Safety, Institute of Mountain Hazards and Environment, Chinese Academy of Sciences, Chengdu, 610299, China
- <sup>b</sup> University of Chinese Academy Sciences, Beijing, 100049, China
- <sup>c</sup> Sichuan Province Engineering Technology Research Center of Mountain Hazard Mitigation, Chengdu, 610299, China

#### ARTICLE INFO

# Article history: Received 17 October 2023 Received in revised form 3 July 2024 Accepted 12 July 2024 Available online 22 July 2024

Keywords:
Debris flow
Check dam
Sediment trapping effect
Landform evolution

#### ABSTRACT

Check dams have been used worldwide for a variety of purposes. With increasing age, check dams gradually lose their sediment trapping function via the continuous deposition of material carried by debris flows and flash floods, and eventually, check dams become unable to perform the designed mitigation function. In this paper, the sediment deposit evolution in a dam with multiple debris flow surges and its influence on the sediment trapping effect were investigated. The results showed that the debris flow deposition process can be divided into three phases: the backwater-controlled deposition phase, landform-controlled deposition phase, and quasi-equilibrium phase. The sediment trapping ratio of the check dam gradually decreased as the deposit volume increased and was linearly negatively correlated with the sediment deposition rate. Moreover, a mathematical model describing the negative feedback between deposit volume and sediment trapping ratio was established, and the physical meanings of the coefficients in the model and their empirical values were clarified. Furthermore, the deposit distribution, which satisfied the Weibull distribution in the longitudinal direction, was revealed. In the cross-sectional direction, the distribution of deposition gradually became uneven with increasing sediment filling rate.

© 2024 International Research and Training Center on Erosion and Sedimentation, China Water and Power Press, and China Institute of Water Resources and Hydropower Research. Publishing services by Elsevier B.V. on behalf of KeAi Communications Co. Ltd. This is an open access article under the CC BY-NC-ND license (http://creativecommons.org/licenses/by-nc-nd/4.0/).

#### 1. Introduction

Check dams are widely used as engineering structures and play an important role in debris flow hazard mitigation (Abbasi et al., 2019; Chen et al., 2015; Huebl & Fiebiger, 2005; Lucas-Borja et al., 2021; Piton et al., 2017). One of the main functions of check dams is to trap solid material in debris flows and reduce impacts downstream (Huebl & Fiebiger, 2005; Piton & Recking, 2016a, 2016b; Takahiro et al., 2013). The deposition of debris flows in a check dam can occur layer by layer upstream (Armanini & Larcher,

2001; Piton & Recking, 2016a; Schwindt et al., 2017), which is controlled by temporary deposition and re-entrainment of sediment (Hairsine et al., 2002; Huang et al., 1999; Pudasaini & Krautblatter, 2021; Van Oost et al., 2004). However, check dams gradually lose their sediment trapping effect with continuous sediment deposition (Castillo et al., 2007; Lucas-Borja et al., 2021; Ran et al., 2021) and may even experience partial or full destruction during large-scale debris flow events (Alcoverro et al., 1999; Liu et al., 2020; Robichaud et al., 2019; Vaezi et al., 2017).

Check dams can effectively reduce debris flow velocities and channel bed slopes (Chen et al., 2016; Sun et al., 2018; Zhou et al., 2019a), thereby reducing dynamic action and accelerating deposition. The channel bed slope is an important parameter for describing depositional landforms, and the slope of the final depositional landform (quasi-equilibrium phase) is called the deposition slope (Chen et al., 2016; Piton & Recking, 2016a). The deposition slope is used to calculate the volume of debris flow

<sup>\*</sup> Corresponding author. State Key Laboratory of Natural Hazards and Engineering Safety, Institute of Mountain Hazards and Environment, Chinese Academy of Sciences, Chengdu, 610299, China.

E-mail addresses: chenjg@imde.ac.cn (J. Chen), wangxian@imde.ac.cn (X. Wang), hychen@imde.ac.cn (H. Chen), wyzhao@imde.ac.cn (W. Zhao), wangchenyuan@imde.ac.cn (C. Wang), xqchen@imde.ac.cn (X. Chen).

deposits in a check dam (Huang et al., 2021; Wu et al., 1993, pp. 293-294), and it is mainly affected by the debris flow density, channel slope, spillway position and shape, and other factors (Chen et al., 2016; Piton & Recking, 2016a). Several calculation methods have been proposed based on field observation data, experimental data, and sediment transport models (Armanini & Larcher, 2001: Osti & Egashira, 2013; Schwindt et al., 2018; Wu et al., 1993, pp. 293-294; You et al., 2013). Moreover, numerical simulation methods have also been used to study the evolution of depositional landforms in check dams and have achieved satisfactory results in the back-calculation of field and experimental cases (Bernard et al., 2019; Liu et al., 2013; Mergili et al., 2020; Shrestha et al., 2008; Van Oost et al., 2004). However, there are shortcomings in the simulation of landform details, such as the distribution of sediment deposits in the horizontal and vertical directions (Castillo et al., 2014; Mergili et al., 2020; Shrestha et al., 2008). Most previous studies on the sediment trapping ratio have focused mainly on the influence of discharge orifice type and size (Campisano et al., 2014; Goodwin & Choi, 2020; Ishikawa et al., 2014; Li et al., 2019; Marchelli et al., 2020), while the influence of reservoir landform evolution on the sediment trapping ratio of check dams remains unclear. Therefore, it is necessary to carry out physical model tests to deepen our understanding of landform evolution in check dams and the decline in the ability of check dams to trap sediment.

The feedback effect between the sediment trapping of a check dam and depositional landforms in reservoirs is still in the qualitative description stage, which is not conducive to the efficacy evaluation and maintenance of check dams during their operation phase. The purpose of this paper is to illuminate the evolution of depositional landforms in check dam reservoirs and the effect on the sediment trapping ratio of check dams. To achieve this purpose, physical flume experiments involving multiple debris flow surges were carried out.

# 2. Materials and methods

# 2.1. Experimental setup

The experiments were conducted at the Dongchuan Debris Flow Observation and Research Station, Chinese Academy of Sciences, Yunnan, China. The test device consisted of material buckets, a hopper, a flume, a check dam, and tailings buckets (Fig. 1). The material buckets were used to soak, stir, and store the debris flow

mixture, and the mixture consisted of water and deposited sediment samples from Jiangjia Gully, Yunnan. The mass of the water was determined by that of the deposited sediment sample and the designed density of the debris flow in this flume experiment  $(1300 \text{ kg/m}^3)$  and  $1500 \text{ kg/m}^3)$ .

Before the experiments, the mixture was transferred from the material bucket to the hopper, and the hopper was used to temporarily store the mixture and deliver debris flows into the flume. The valve between the hopper and flume was used to control the debris flow discharge. The flume had a rectangular cross-section with Plexiglas on two sidewalls, and its length, width ( $B_f$ ), and height were 7.0 m, 0.4 m, and 0.4 m, respectively. The slope of the test flume bed ( $S_{\rm init}$ ) was 20%, which is within a reasonable range and based on a field test (Rickenmann, 1999). Fig. 1 also shows the three types of check dam models that were used in the experiments. The check dams had widths (B) of 0.40 m and heights (H) of 0.15, 0.10 and 0.05 m, respectively. Tailings buckets were placed at the end of the flume to collect debris flow material passing through the check dam.

# 2.2. Materials and applicability

Some dimensionless parameters were controlled, and the test design was based on the general conditions of field cases. The Froude number (Fr) was considered because a debris flow is a gravitational process with open channel flow characteristics, and the Fr values of the debris flows in the experiments were measured in the range of 4.0–5.5, which are comparable to those of field and experimental cases (Choi et al., 2015; Du et al., 2023; Song et al., 2021; Zhou et al., 2019a). In addition, the H/B ratios of the check dam models (Fig. 2) were 0.125, 0.250, and 0.375, which are reasonable compared with those of check dams constructed in the Minjiang Basin (0.029–0.400), Sichuan, China.

Two types of debris flows, with  $C_{\rm V}=0.18$  and 0.30, were used in the tests, where  $C_{\rm V}$  is the sediment concentration and sediment volume fraction (Church & Jakob, 2020; Kaitna & Huebl, 2013). Each material bucket (Fig. 1) contained 21 kg of granular material (sediment) mixed with different volumes of water to form a debris flow mixture with volumes of 4.39 and  $2.63 \times 10^{-2} \, {\rm m}^3$  for the two different debris flow types (Fig. 2). The granular material used in the tests was obtained from the debris flow fan in the Jiangjia gully. Similar to previous experimental conditions (Chen et al., 2017, 2018; Cui et al., 2015; Li et al., 2019), Fig. 2 shows the grain size

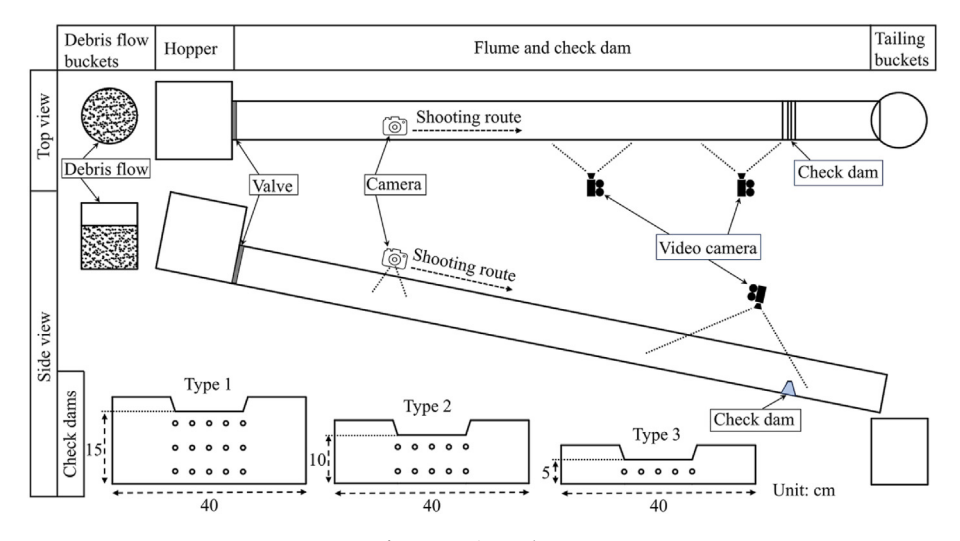


Fig. 1. Experimental setup.

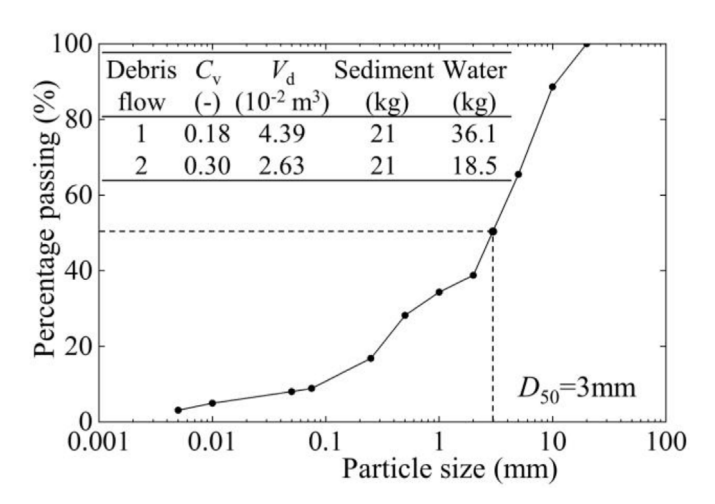


Fig. 2. Compositions of the debris flows.

**Table 1** Experimental arrangement and test conditions.

Case	Check dam height (H)	Debris flow	
		$C_{\rm v}$	Total surges (N)
Case 1	0.15 m	0.18	10
Case 2	0.10 m	0.18	8
Case 3	0.05 m	0.18	8
Case 4	0.15 m	0.30	10
Case 5	0.10 m	0.30	8
Case 6	0.05 m	0.30	8

distribution of the granular material for the tests. The measured density of the granular material was  $\rho_s=2680~\text{kg/m}^3$ , and that of the granular material was  $39.9^\circ$ .

#### 2.3. Experimental design and measured variables

Table 1 shows the experimental design and test conditions. There were 6 cases based on the different check dams and  $C_v$  values. Each case included 8 or 10 debris flow surges that were named S1 to S8 or S10, respectively, and the time interval between adjacent debris flows was 240 s. Between debris flow events, the morphological characteristics of the sediment deposits behind the check dam reservoir were recorded by a camera (Nikon D850,  $6016 \times 4016$  pixels, f = 24 mm), and photogrammetry was used to obtain digital elevation models (James & Robson, 2012; Qin et al., 2018). Then, the volume and distribution of the deposits were determined by comparing different digital elevation models (Cucchiaro et al., 2019). The deposition process was recorded by a video camera (GoPro hero7 Black, 4096 × 2160 pixels, 25 fps) on the top of the flume (Fig. 1). The velocity and depth of the debris flow and the deposition process were recorded by two video cameras (SONY FDR-AX60, 4096 × 2160 pixels, 25 fps) on the side of the flume with the help of large tracer particles (Fig. 1). Finally, the mass ( $m_{tail}$ ) and volume ( $V_{tail}$ ) of the tailings of each debris flow were measured, and the mass  $(m_{out})$  of the granular material in the tailings was calculated as follows:

$$m_{out} = \frac{\rho_s(m_{tail} - \rho_w V_{tail})}{\rho_s - \rho_w} \tag{1}$$

where  $\rho_s$  and  $\rho_w$  are the densities of the granular material and water, respectively, with values of  $\rho_s=2680~{\rm kg/m^3}$  and  $\rho_w=1000~{\rm kg/m^3}$ .

#### 2.4. Parameters and dimensional analyses

Here, we listed the parameters and their meanings in this study. In addition, we established some of the dimensionless parameters based on previous studies for comparison, discussion, and engineering applications, which are listed in Table 2.

**Table 2** Parameters and meanings.

Parameters and units	Meanings	Parameters and units	Meanings
b (m)	the distance between any point in the deposits and the left sidewall of the flume		the accumulated volume of $n$ debris flow surges
$B\left(B_{\mathrm{f}}\right)\left(\mathrm{m}\right)$	the width of the check dam (flume)	$V_{\rm d}~({ m m}^3)$	the volume of a debris flow surge
$C_{v}(-)$	the debris flow sediment concentration	$V_{\rm dep}~({ m m}^3)$	the volume of the deposits
H (m)	the effective height of the check dam	$V_{\rm dep,i}~(\rm m^3)$	the volume of deposition during the i-th debris
			flow surge
<i>L</i> (m)	the distance between any point in the deposits and the upstream edge of the check dam	$\rho_{\rm d}  ({\rm kg/m^3})$	the stored sediment dry density
$m_{\rm in}$ (kg)	the total mass of granular material in a debris flow surge (in the material bucket)	$\rho_{\rm s}$ (kg/m <sup>3</sup> )	the granular material density
m <sub>out</sub> (kg)	the mass of granular material passing through a check dam in a debris flow surge (in the tailings)	: H∗	the relative height of the check dam
n (-)	the accumulated number of debris flow surges	V*	the relative accumulated volume of $n$ debris flow surges
N (-)	the maximum number of debris flow surges	ω	the sediment trapping ratio
$S_{\text{dep}}(-)$	the deposition slope	$\phi$	the sediment filling rate of the check dam reservoir
$S_{\text{init}}(-)$	the initial slope of the channel bed		

Note:  $V_D = nV_{\rm d}$ ;  $V_{dep} = \sum_1^n V_{dep,i}$ ;  $\rho_{\rm d}$  is measured to be approximately 1786 kg/m³ and 1975 kg/m³ for  $C_{\rm v} = 0.18$  and 0.30, respectively;  $\rho_{\rm s} = 2680$  kg/m³. Based on previous research, dimensionless parameters that are convenient for reference in engineering practice were constructed:  $H_* = H/B$ ;  $V_* = V_D/B_f^3$ ,  $B_f^3$  is the volume scale used in this study (Wang et al., 2022, 2024). In this study, a debris flow surge is used as a unit of measurement, and the calculation method for  $V^*$  is  $V_* = nV_d/B_f^3$ ;  $\omega = [\rho_d \cdot \Delta(V_{dep})]/[C_v \cdot \rho_s \cdot \Delta(V_D)]$  is the sediment trapping ratio, which is the ratio of the granular material mass deposited in a check dam reservoir to that entering the reservoir;  $\Delta$  is the difference operator, and a similar parameter was utilized by Li et al. (2019), Schwindt et al. (2018), and Sun et al. (2018). In this study, a debris flow surge is used as a unit of measurement, and the measured value is  $\omega = 1 - m_{out}/m_{in}$ ;  $\phi = V_{dep}/V_0$  is the sediment filling rate of the check dam reservoir, which is obtained by the ratio between the deposit volume and the basic reservoir storage capacity ( $V_0 = H^2B_f/(2S_{init}V_{dep,i})/(H^2B_f)$ ), and similar parameters were employed by Lien (2003), Lucas-Borja et al. (2018), and Ran et al. (2021). In this study, the calculation method of  $\phi$  is  $\phi = \sum_{i=1}^n [(2S_{init}V_{dep,i})/(H^2B_f)]$ . y = L/H represents coordinates in a linear coordinate system using the upstream edge of the check dam as the coordinate origin, taking H as the unit length, and setting the upstream horizontal direction as positive.

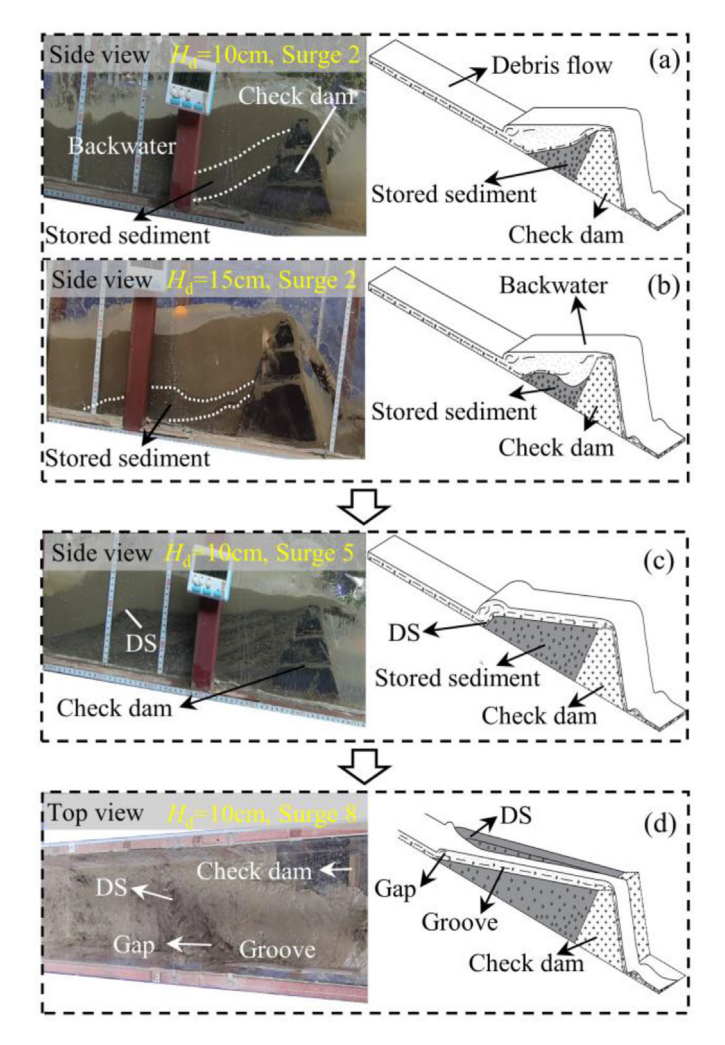


**Fig. 3.** Deposition process of debris flows in a check dam. (a) the backwater-controlled deposition phase (dam height is 10 cm); (b) the backwater-controlled deposition phase (dam height is 15 cm); (c) the landform-controlled deposition phase; (d) the quasi-equilibrium phase.

# 3. Results and analysis

# 3.1. Deposition process behind the check dam reservoir

The check dam changed the debris flow velocity and reduced the channel slope in the reservoir area, which caused a large amount of deposition. Fig. 3 shows that the deposition process behind the check dam reservoir could be divided into three phases: the backwater-controlled deposition phase (Fig. 3(a) and (b)), the landform-controlled deposition phase (Fig. 3(c)), and the quasiequilibrium phase (Fig. 3(d)). During the phase of backwatercontrolled deposition, debris flow deposition was significantly affected by the backwater behind the check dam reservoir. Similar phenomena were reported by Piton & Recking (2016) and Armanini & Larcher (2001). The deposition volume was mainly affected by the particle deposition velocity, the length of the backwater area, and the flow velocity. The dam height directly affected the depth and length of the backwater and further affected the debris flow velocity and deposition process. The backwater depth and length were relatively small at H = 0.10 m, the debris flow velocity was relatively high, and the sediment-laden capacity was strong enough to shape temporarily deposited sediment into a smooth

reverse slope upstream of the check dam (Fig. 3(a)). When H=0.15 m, the backwater depth and length were relatively large, and the deposition was concentrated away from the check dam (Fig. 3(b)). With the continuous deposition of sediment, the deposit depth reached the dam height. Then, debris flows did not directly impact the check dam but directly impacted the sediment deposit. The deposition entered the landform-controlled phase.

During the phase of landform-controlled deposition, a deposition scarp (DS) formed at the end of the sediment deposition process and acted as a dam (Fig. 3(c)). This phenomenon was caused by the concentrated energy dissipation of the debris flow at the end of sediment deposition and the sediment-carrying function. When debris flows passed through the DS, the depth increased, and the velocity decreased. In addition, when debris flows passed through the sediment deposit, deposition also occurred because the sediment deposition slope was lower than the initial channel slope. As sediment deposition progressed, the deposition entered the quasiequilibrium phase. During the quasi-equilibrium phase, the DS height was low, which weakened the energy dissipation effect around the DS. In addition, the debris flows created a rill with good hydraulic conditions on the deposit surface (Fig. 3(d)), which made the debris flow pass through the deposits and check dam smoothly and weakened the sediment deposition in the reservoir. Temporary deposition and re-entrainment of sediment reached a dynamic balance. A quasi-equilibrium state was gradually reached when the debris flow scale stabilized.

Fig. 4 describes the evolution of the sediment deposits behind the check dam with Case 2 as an example, where b is the distance from the left sidewall of the flume,  $A_{dep}$  is the area of the longitudinal deposit section, and R is the topographic relief in the cross section. Fig. 4(a) shows the evolution of landforms along the longitudinal section; Fig. 4(b) shows the evolution of sediment deposits along a cross-section (Section 1-1 in Fig. 4(a)); Fig. 4(c) shows the uneven distribution of sediment deposits in the direction perpendicular to the channel. Along the longitudinal section of the flume, the sediment deposits developed layer by layer upstream, and a DS on the upstream side of the sediment deposits was obvious. The sediment deposition volume of an individual surge tended to decrease with deposit development, and its distribution was uneven and mainly concentrated on the upstream side (Fig. 4(a)). At the initial stage of sediment deposition (S1 and S2), the deposition was uneven in Section 1-1 (Fig. 4(b)), but from the perspective of the whole depositional area, there was no significant uneven distribution of sediment deposits (Fig. 4(c)). The uneven distribution shown in Fig. 4(b) may be due to the measurement error of photogrammetry caused by the backwater. As sediment deposition continued, the uneven distribution of sediment deposits in the cross-sectional direction increased (S3 to S8 in Fig. 4(c)) because the debris flow gradually formed a rill on the deposit surface (S3 to S8 in Fig. 4(b)). Contrary to other places, in this rill, a deeper flow, larger base shearing force, stronger re-entrainment effect, and greater re-entrainment depth occurred. This effect continuously enhanced the difference in sediment deposition in the cross-section and finally formed and maintained the rill. The rill caused the debris flows to move along one side of the channel and to discharge from the dam abutment (Fig. 3(d)).

# 3.2. Sediment trapping ratio and deposit volume

In the feedback system between the depositional landform in the reservoir and the sediment trapping effect of the check dam, the deposit volume ( $V_{\rm dep}$ ) and sediment trapping ratio ( $\omega$ ) were studied as the main variables. In addition,  $\omega$  and  $\phi$  have a linear correlation:

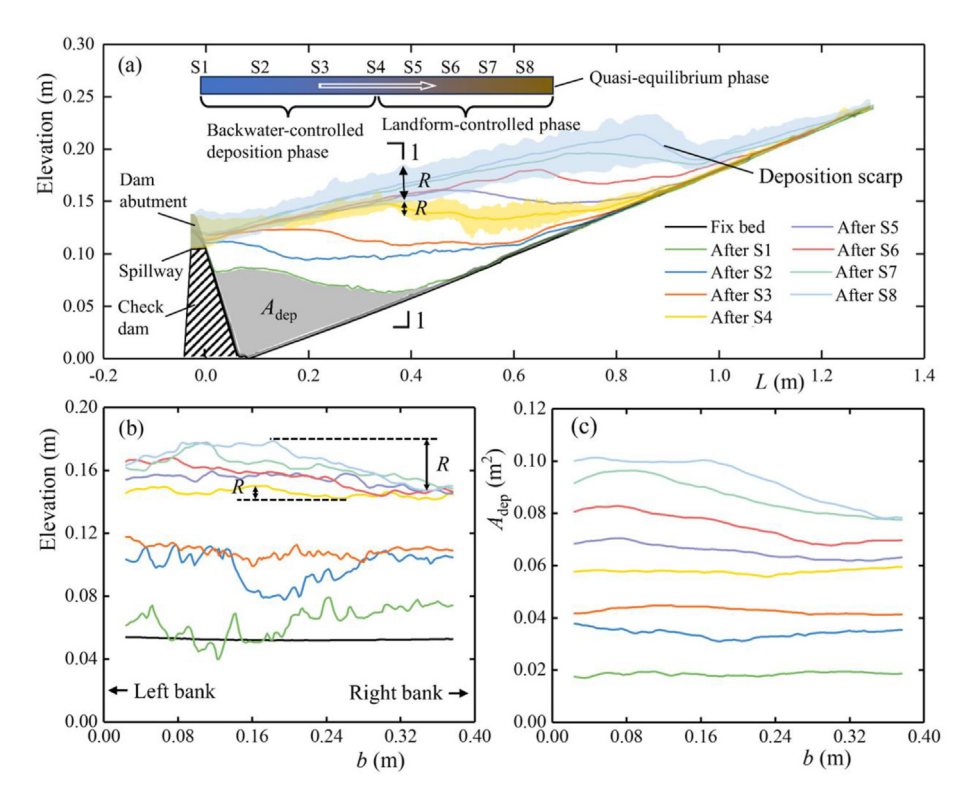


**Fig. 4.** Evolution of the sediment depositional landform behind the check dam (Case 2). (a) The evolution of the sediment deposits along a longitudinal section; (b) the evolution of the sediment deposits along a cross-section. The solid line in Fig. 4(a) is the average elevation, and the shaded part is the range of elevation. (Note: b is the distance from the left sidewall of the flume,  $A_{\text{dep}}$  is the area of the longitudinal deposit section, and R is the topographic relief in the cross-section).

$$\omega = \omega_0 - k\phi \tag{2}$$

where  $\omega_0$  is the sediment trapping ratio when the check dam reservoir is empty (initial sediment trapping ratio) (dimensionless parameter), k is the attenuation rate of  $\omega$  (dimensionless parameter),  $\phi$  is the sediment filling rate (dimensionless parameter), and  $\omega_0/k$  is the maximum filling rate ( $\phi_{\rm max}$ ), which appears in the quasiequilibrium phase. With increasing  $\phi$ , theoretically,  $\omega$  gradually decreases from  $\omega_0$  to 0, and  $\phi$  gradually increases from 0 to  $\phi_{\rm max}$ . In this study, the values of  $\omega_0$  and k were measured to be 0.806 and 0.819 and 0.136 and 0.107 for  $C_{\nu}=0.18$  and 0.30, respectively. The sediment trapping ratio  $\omega$  is the ratio of the granular material mass deposited behind the check dam reservoir to that entering the reservoir:

$$\omega = \frac{\rho_d}{\rho_s \cdot C_v} \cdot \frac{\Delta \left( V_{dep} \right)}{\Delta \left( V_D \right)} \tag{3a}$$

where  $\Delta$  is the difference operator, and a similar parameter was utilized by Li et al. (2019), Schwindt et al. (2018), and Sun et al. (2018). In this study, a debris flow event was used as the unit of measurement, and the measured value was  $\omega = 1 - m_{out}/m_{in}$ . Substituting  $V_{\rm dep} = \phi V_0$  and  $V_{\rm D} = V^*/B_{\rm f}^{\rm f}$  into Eq. (3a) and combining Eq. (2) and Eq. (3a) yields the following:

$$\frac{\rho_d \cdot V_0}{\rho_s \cdot C_v \cdot B_f^3} \cdot \frac{\Delta(\phi)}{\Delta(V_*)} = \omega_0 - k\phi \tag{3b}$$

The above formula can be transformed into the following:

$$\frac{\partial(\phi)}{\partial(V_*)} = \frac{2S_{init}}{H_*^2} \cdot \frac{\rho_s \cdot C_v}{\rho_d} (\omega_0 - k\phi)$$
 (3c)

Substituting  $t = \frac{2S_{init}}{H_*^2} \cdot \frac{\rho_s \cdot C_v}{\rho_d}$  into Eq. (3c), and solving the differential equation (Eq. (3c)), we obtain:

$$\phi = \frac{\omega_0}{L} (1 - \exp(-tkV_*)) \tag{4}$$

Thus, the following formula for calculating the deposit volume is

$$V_{dep} = \frac{\omega_0}{k} (1 - \exp(-tkV_*)) \cdot V_0 \tag{5}$$

Fig. 5 shows the sediment trapping ratio and deposit volume, where  $V^*$  is the relative accumulated volume of the debris flow,  $V_{\rm dep}$  is the volume of the deposit,  $\omega$  is the sediment trapping ratio, and  $\phi$  is the sediment filling rate of the check dam reservoir. Fig. 5(a) shows that  $\omega$  is positively correlated with the relative height  $(H^*)$  of the check dam because as the relative height of the check dam decreases, the length and depth of the backwater in the reservoir decrease, the energy dissipation effect decreases, the debris flow velocity increases, the temporary sediment deposition volume decreases, and the sediment re-entrainment volume increases, which decreases  $\omega$ . Fig. 5(b) shows that  $\omega$  is negatively correlated with V\* because as V\* increases, the check dam reservoir gradually becomes filled with stored sediment. The slope of the deposit surface and the debris flow velocity gradually increase, which reduces the volume of temporary deposition and strengthens the re-entrainment effect. Overall, the abovementioned two reasons lead to a reduction in the net deposition volume and  $\omega$ . Fig. 5(c) and d shows that  $\omega$  is negatively correlated with the filling rate  $(\phi)$ , which means that as  $\phi$  increases, the

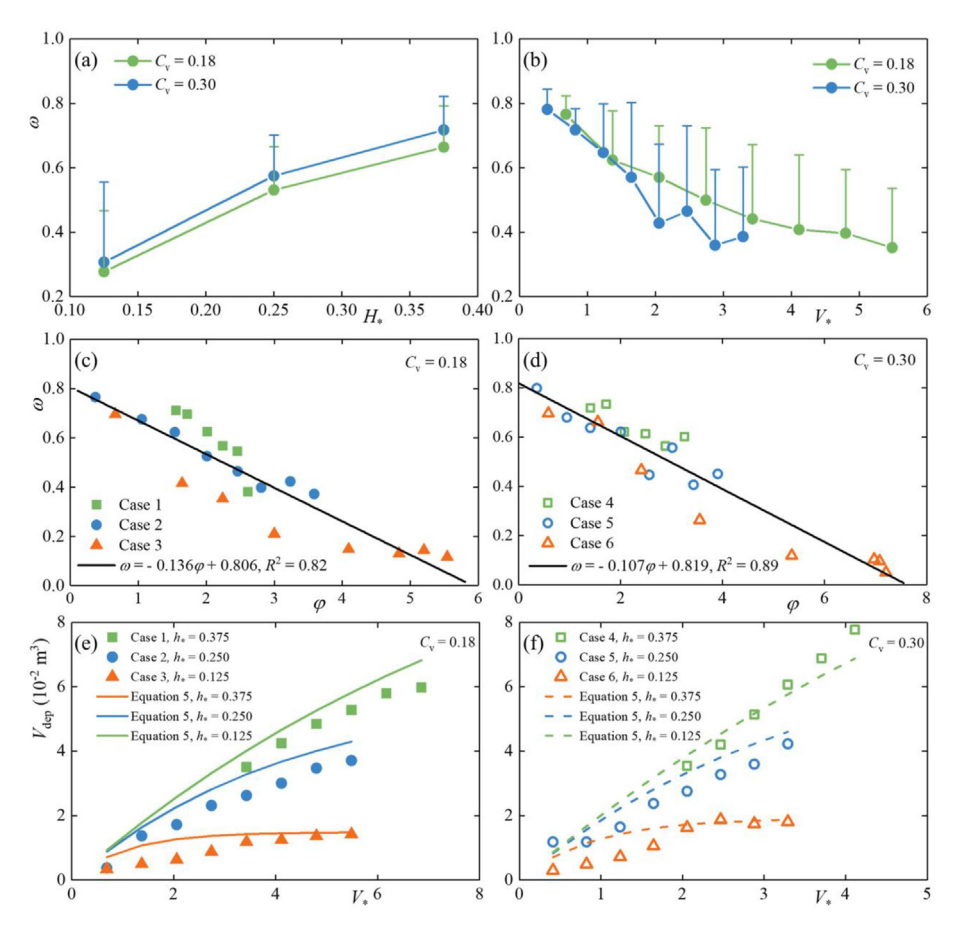


**Fig. 5.** Sediment trapping ratio and deposit volume. (a) and (b) The impact of relative dam height  $(H^*)$  and relative cumulative volume of debris flow  $(V^*)$  on sediment trapping ratio  $(\omega)$ ; (c) and (d) The relationship between sediment trapping ratio and the sediment filling rate  $(\phi)$  of check dam reservoir under conditions of debris flow with  $C_v = 0.18$  and 0.3, respectively; (e) and (f) Comparison of measured and calculated the volume of deposition  $(V_{dep})$  under conditions of debris flow with  $C_v = 0.18$  and 0.3, respectively. (Note: Whiskers in (a) and (b) signify the standard deviation,  $H^*$  is the relative height of the check dam). c) 3.3 Distribution characteristics of sediment deposition.

deposition volume decreases for the same reason as mentioned in the previous paragraph. Fig. 5(e) and f shows the comparison of the calculated and experimental values of  $V_{\rm dep}$ , which indicate that the calculated values are slightly larger than the experimental values. This is because a small amount of sediment remaining in the material bucket, hopper and flume was calculated as part of  $\omega$ . Eq. (5) integrally describes the deposition process of the sediment volume with a small error, which provides a new method to calculate  $V_{\rm dep}$  considering the decreasing efficacy of a check dam in trapping sediment for debris-flow mitigation design.

To quantitatively interpret the distribution characteristics of the sediment deposits along the longitudinal direction of the flume, we analysed the probability distribution characteristics of the longitudinal position (*Y*) of the sediment deposits and described it with the Weibull distribution:

$$F(y) = 1 - e^{-\left(\frac{y}{\eta}\right)^{\beta}} \tag{6}$$

where  $\eta$  is the scale parameter, and  $\beta$  is the shape parameter. The Weibull distribution was selected for its good fit ( $R^2 = 0.997 \pm 0.001$ ) with Y (Fig. 6(b)).

Taking Case 2 as an example, Fig. 6(a) shows the development process of the deposits behind the check dam reservoir, and Fig. 6(b) shows the cumulative distribution curve of Y and the fitted Weibull distribution curve. Fig. 6(c) and d shows the values of  $\beta$  with  $C_V=0.18$  and 0.30, respectively. The average values of  $\beta$  were

1.605 and 1.549, and the standard deviations of the  $\beta$  values were 0.049 and 0.045, respectively. The influence of  $C_v$  on  $\beta$  was significant because the two-tailed p value in Student's t-test was 0.0004 (<0.05). The correlation between  $\beta$  and  $\phi$  was minimal, and the correlation coefficients were r = 0.26 and 0.54 (<0.6) for debris flows with  $C_v = 0.18$  and 0.30, respectively. Fig. 6(e) and f shows the values of  $\eta$  when  $C_v = 0.18$  and 0.30, respectively, and  $\eta$  was linearly positively correlated with  $\phi$ . This indicates that as  $\phi$  increases, the distribution of deposits becomes more dispersed in the longitudinal direction. Under the condition of the same  $\phi$ , the distribution of sediment deposits of a debris flow with  $C_{\rm v} = 0.30$  as more dispersed than that of a debris flow with  $C_{\rm v}=0.18$ , which is caused by the influence of  $C_v$  on the deposition pattern: with the increase in  $C_v$ , the deposition development pattern gradually changes from downstream to upstream (Figs. 4(a) and 8(b)) to bottom to top (Fig. 8(c)).

To quantify the uneven distribution of deposits in the crosssectional direction, the following parameter is proposed:

$$D = \frac{SD(A_{dep})}{HB_f} \tag{7}$$

where D is the coefficient of the topographic relief in the cross-section (-), and H represents the deposition length for the good proportional relationship between them (m).

Fig. 7 shows that D is positively correlated with  $\phi$  because as  $\phi$ 

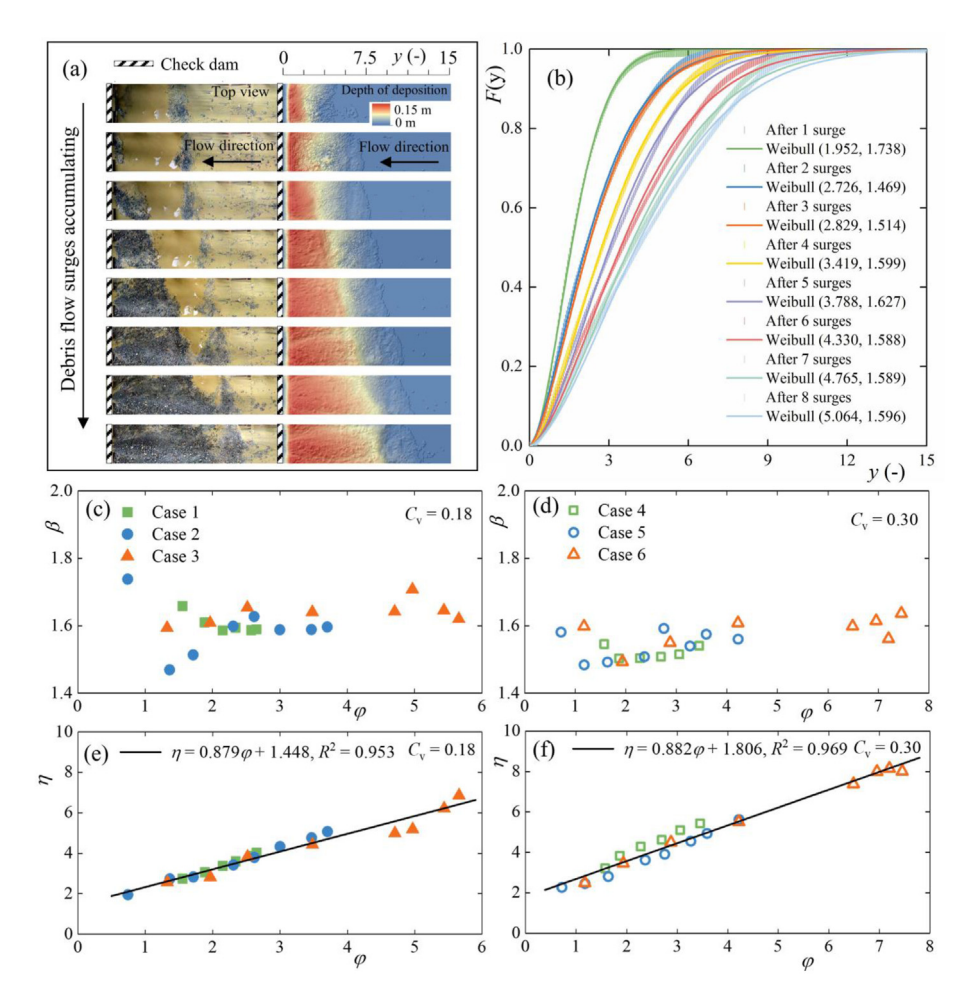


**Fig. 6.** Longitudinal distribution of the deposits behind the check dam reservoir. (a) Development and distribution of deposits (Case 2), (b) the cumulative distribution curve of Y and the fitted Weibull distribution curve (Case 2), (c) and (d) the values of the shape parameter when  $C_v = 0.18$  and 0.30, respectively, and (e) and (f) the values of the scale parameter when  $C_v = 0.18$  and 0.30, respectively.  $\phi$  is the sediment filling rate of the check dam reservoir.

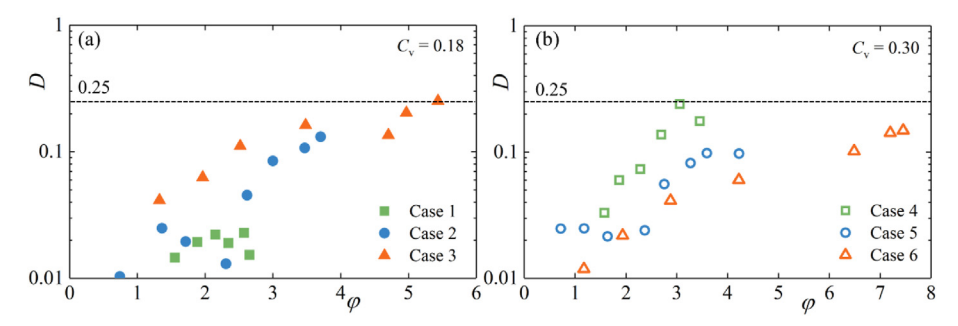


Fig. 7. Evolution of the coefficient of topographic relief in the cross-section (D) under various test conditions. (a)  $C_v = 0.18$  and (b)  $C_v = 0.30$ .

increases, the re-entrainment effect of the debris flow is enhanced. The depth of the groove and the uneven distribution of the base shearing force in the cross-section form a positive feedback cycle, which maintains and enhances the groove and uneven distribution of deposition. In addition, *D* is also affected by the check dam height and sediment concentration. The maximum value of *D* may be a great reference for designing the dam abutment height (spillway depth) to prevent debris flows from climbing over the dam abutment. Specifically, the cross-section of the channel, the flow section and flow parameters, and the risk of debris flows crossing the dam

abutment can be evaluated in sequence, and the results show that the maximum value is D = 0.25.

## 4. Discussion

This study is dedicated to revealing the evolution of the depositional landforms in a check dam and the decline in the sediment trapping efficacy of check dams impacted by debris flows. The experimental results showed that the sediment deposition process of debris flows in a check dam can be divided into three phases: the

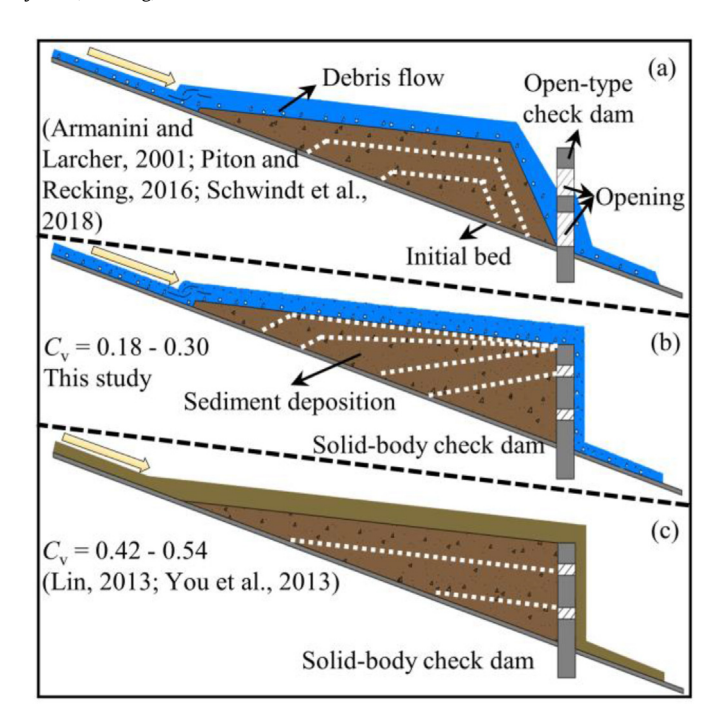


**Fig. 8.** Sediment deposition process in check dams. (a) Evolution process under diluted debris flow and open-type check dam conditions, (b) evolution process under diluted debris flow and solid-body check dam conditions, and (c) evolution process under viscous debris flow and solid-body check dam conditions.

backwater-controlled deposition phase, the landform-controlled deposition phase, and the quasi-equilibrium phase. They also showed that the sediment trapping ratio of a check dam was linearly negatively correlated with the sediment filling rate, and a new sediment deposition volume calculation method considering the evolution of  $\omega$  was proposed, as shown in Eq. (5), which together formed a feedback model. Notably, the selected factors of the experimental conditions were typical and representative, but we ignored the influence of soil particle properties on debris flow, which meant that the particle size distribution, soil category, pore size, etc., were also important. Meanwhile, debris flows and floods in real-world gullies may occur alternately, and their volumes are also variable. Therefore, the results of this study need more

verification and correction before use in the maintenance and desilting plans of check dams.

This experimental study was carried out under conditions of debris flows with  $C_v = 0.18$  and 0.30 and closed-type check dams. As shown in Fig. 1, the openings were only used to dissipate pore water pressure, and the sediment deposition evolution process is summarized in a schematic diagram (Fig. 8(b)). In real-world gullies, the sediment deposition evolution process in check dams is also affected by the dam opening type, size, and sediment concentration (Campisano et al., 2014; Han & Ou, 2006; Schwindt et al., 2017; Wang et al., 2019). When the opening size is large enough (Fig. 8(a)), a debris flow can discharge smoothly through the openings and form little backwater. Sediment deposition is mainly controlled by mechanical blocking of the discharge orifices, and deposits form layer by layer (Armanini & Larcher, 2001; Piton & Recking, 2016a; Schwindt et al., 2018). The slope is influenced by temporary sediment deposition and re-entrainment (Hairsine et al., 2002; Van Oost et al., 2004). With a large enough C<sub>v</sub>, a debris flow can be regarded as a one-phase flow, and the deposition is in the form of overall stagnation rather than solid-liquid separation. As shown in Fig. 8c, the deposits grow layer by layer with a certain slope, which is affected by the material characteristics of the debris flows, such as grain size, rheology, and internal friction angle (Chen et al., 2016; De Haas et al., 2015; Major & Iverson, 1999; You et al., 2013: Zhou et al., 2019b). In addition, the Froude number is also one of the main factors influencing the interaction between check dams and debris flows (Choi et al., 2015; Faug, 2015; Kaitna & Huebl, 2013: Li et al., 2021: Ng et al., 2019).

A model of the sediment trapping ratio and deposit volume was constructed in which the initial value ( $\omega_0$ ) and attenuation coefficient (k) of  $\omega$  are important parameters. This study also provided empirical values based on experimental data with a limited range of applications. Previous studies on  $\omega$  have focused on the conditions of  $\phi=0$ , and the results can be used to estimate  $\omega_0$ . The sediment deposition slope ( $S_{\rm dep}$ ) is an equilibrium slope, and  $\phi$  reaches the maximum value when  $\omega=0$  ( $\phi_{\rm max}=\omega_0/k$ ). With the conditions that the deposits reach the height of the check dam and its surface is smooth, the relationships between  $\phi_{\rm max}\sim S_{\rm dep}$  and  $k\sim S_{\rm dep}$  are  $\phi_{\rm max}=1/(1-S_{\rm dep}/S_{\rm init})$  and  $k=\omega_0$  (1- $S_{\rm dep}/S_{\rm init}$ ), respectively. Therefore, contrary to Eqs. (2) and (5), previous studies on  $\omega$  and  $S_{\rm dep}$  may expand the application range, and  $\omega_0$  is affected by the type of check dam, material composition, debris-flow velocity, and initial channel slope (Li et al., 2019; Schwindt et al., 2018; Shima

**Table 3** Methods for calculating  $\omega_0$ , the sediment trapping ratio when the check dam reservoir is empty (initial sediment trapping ratio).

Reference	Formulas and values <sup>b</sup>	Applicability <sup>a</sup>
Ishikawa et al. (2004, 2014)	0-0.800	The values are suitable for steel open-type check dams under water-rock flow. The rate of pipe interval to maximum particle size is from 3.0 to 1.5.
	$\omega_0 = \frac{\sum_{i=1}^{N} (s/d_{50})^{1.40} e^{V^{0.7}}}{(s/d_{50})^{1.40} e^{V^{0.7}}}$	The formula is suitable for slit dams and considers the influence of the number and size of slits, the velocity and particle size of sediment.
Sun et al. (2018)	$\omega_0 = 1.2645 (b/d_{90})^{-0.3965} C_v^{0.6672} F_r^{0.0696}$	The formula is suitable for beam dams and considers the influence of the distance between beams, $C_{\rm V}$ and $Fr$ .
Schwindt et al. (2018)	0.390-0.720	The values are suitable for check dams with an opening and mechanical blocking structures under hyperconcentrated flow.
Li et al. (2019)	$\omega_0 = \frac{0.0906\chi^{0.9638}}{0.0906\chi^{0.9638} - 0.0565 \ ln(59.4867\chi)}$	The formula is suitable for window-check dams and considers the influence of the opening ratio, the size of a window, $C_V$ and $S_{\rm init}$ .
	$\chi = \alpha_0 \left( \frac{A_{drain \; hole}}{A_{dam}} \right)^{\alpha_1} \left( \frac{b}{d_{95}} \right)^{\alpha_2} \left( \frac{h}{b} \right)^{\alpha_3} \left( \frac{\gamma_1}{\gamma_{water}} \right)^{\alpha_4} (\theta)^{\alpha_5}$	
This study	0.806, 0.819	The values are suitable for check dam with small openings under debris flows with $C_{\rm v}=0.18$ and 0.30, respectively.

<sup>&</sup>lt;sup>a</sup> A check dam is a dam with an opening, comprising a basin and an outlet structure. A window-check dam is a check dam with several square openings like windows in its body. A slit dam consists of an array of densely spaced concrete columns. A beam dam is defined as a check dam featuring several horizontally oriented openings within its body, with the width of the openings significantly exceeding their height. (Gong et al., 2021; Li et al., 2019; Piton & Recking, 2016a; Sun et al., 2018).

b The meanings of the parameters in the formulas are detailed in the references.

**Table 4** Method for calculating  $S_{dep}$ .

Reference	Formulas and values <sup>a</sup>	Applicability
Wu et al. (1993)	$\frac{S_{dep}}{S_{init}} = $ $\begin{cases} 0.70 \sim 0.75, H < 5 \text{ m} \end{cases}$	The method is based on field observation data. Eqs. $(1)$ and $(2)$ are suitable for debris flows, and $H$ is the height of check dam. The specific value is recommended to be selected according to the frequency of events: The higher the frequency is, the larger the value.
	$0.60 \sim 0.70, H \in [5, 10] \text{m}$ (1)	
	$0.50 \sim 0.60, H > 10 \text{ m}$	
	$0.75 \sim 0.95, H < 5 \text{ m}$	
	$0.70 \sim 0.90, H \in [5, 10] \text{m}$ (2)	
	$0.60 \sim 0.85, H > 10 \text{ m}$	
Armanini and Larcher (2001)	$\begin{cases} 0.75 \sim 0.95, H < 5 \text{ m} \\ 0.70 \sim 0.90, H \in [5, 10] \text{m} \\ 0.60 \sim 0.85, H > 10 \text{ m} \end{cases} $ (2) $S_{dep} = \frac{\chi B}{Q} \left[ \vartheta_{cr} \Delta D + \left( \frac{1}{n} \frac{Q_s \Delta}{R \sqrt{g}} \right)^{2/3} \right]^{3/2}$	The formula is based on a uniform flow equation and a sediment transport equation and is suitable for debris flows with $S_{\rm dep} < 0.04$ .
Takahashi, T. (2009)	$S_{dep} = \tan \theta_{dep} = \frac{C_{\nu}(\rho_{s}/\rho_{w} - 1)}{1 + C_{\nu}(\rho_{s}/\rho_{w} - 1)} \tan \phi$	This formula is applicable to debris flows with low fine particle content, and the internal friction angle of solid particles is adequately accounted for.
You et al. (2013)	$S_{dep} = S_{init} + \frac{\tan \theta - S_{init}}{\tan^2(45^\circ - \theta/2)}$	The formula considers the influence of the internal friction angle of a debris flow and $S_{\text{init}}$ and is suitable for debris flows.
Chen et al. (2016)	$\frac{S_{dep}}{S_{0.9470}} = 0.6041\gamma^{0.0526}$	Debris flows with densities of 1500–2240 kg/m <sup>3</sup> .
Piton and Recking (2016a)	$\frac{S_{dep}}{S_{init}} = 1/2, 2/3$	$1/2$ is for small floods, and $2/3$ is for large floods with a high $C_{\nu}$ .
This study	$\frac{S_{dep}}{S_{init}} = 0.834, 0.869$	The values are suitable for debris flows with $C_{\nu}=0.18$ and 0.30.

<sup>&</sup>lt;sup>a</sup> The meanings of the parameters in the formulas are detailed in the references.

et al., 2016; Sun et al., 2018). Table 3 presents the summarized calculation formulas and values. All of these methods are based on the results of physical model tests and are easy to use in engineering practice.

Table 3 provides essential insights into the primary factors influencing  $\omega_0$ , including the relative opening degree of the check dam, which characterizes the opening size concerning the sediment's characteristic particle size, the sediment concentration and movement characteristics of the debris flow, and the slope of the initial channel bed. Different types of check dam openings necessitate specific adjustments in the calculation of  $\omega_0$ . For windowcheck dams, factors such as window height and the number of windows must be considered (Li et al., 2019). Similarly, for slit dams, consideration should be given to the number of crevices (Silva et al., 2016). In the case of beam dams, the height of the grid is a pivotal parameter (Sun et al., 2018). These nuanced variations in the calculation formula of  $\omega_0$  underscore the importance of accounting for diverse dam configurations, ensuring a comprehensive analysis of their impact. Numerical simulation studies based on hydraulic models and particle flow models can also provide a reference for  $\omega_0$  (Campisano et al., 2014; Goodwin & Choi, 2020; Ishikawa et al., 2014; Marchelli et al., 2020). Sdep is influenced mainly by the initial channel slope, check dam height, material composition, and scale and frequency of debris flows (Armanini & Larcher, 2001; Chen et al., 2016; Piton & Recking, 2016a; Wu et al., 1993, pp. 293-294; You et al., 2013). Some calculation methods for S<sub>dep</sub> are presented in Table 4. Table 4 reveals that the volume concentration of sediment and the initial channel bed ratio of debris flows are pivotal factors affecting  $S_{\text{dep}}$ . These variables typically dominate the suitable calculation formula (Armanini & Larcher, 2001; You et al., 2013). To enhance the universality of the calculation formula, extensive research data have been consolidated, leading to the development of more applicable calculation methods (Chen et al., 2016). The numerical simulation method can

also provide a reference for  $S_{\rm dep}$  (Bernard et al., 2019; Liu et al., 2013; Shrestha et al., 2008; Van Oost et al., 2004). The results of this paper combined with those of previous studies could be a preliminary reference for determining the sediment trapping ratio and deposit volume in check dams.

#### 5. Conclusions

This paper studied the landform evolution process in a check dam reservoir and its influence on the trapping of sediment from debris flows by check dams. Based on the experimental results, the main conclusions are as follows.

- (1) The sediment deposition process in a check dam can be divided into three phases: the backwater-controlled deposition phase, the landform-controlled deposition phase, and the quasi-equilibrium phase. The sediment trapping ratio was positively correlated with dam height, negatively correlated with the accumulated debris flow volume, and linearly negatively related to the sediment filling rate of the dam reservoir. With increasing deposition behind the check dam, the sediment trapping ratio gradually decreased.
- (2) A mathematical model describing the negative feedback between the reservoir deposit volume and the sediment trapping ratio was developed, which considers the effects of many selected factors, such as the check dam height, channel landforms, material composition of the debris flow and stored sediment, volume of the debris flow, and initial value and attenuation coefficient of the sediment retention rate. Regarding the debris flows with sediment concentrations of  $C_V = 0.18$  and 0.30, their declines in sediment-trapping efficacy were 0.136 and 0.108, respectively.
- (3) The longitudinal distribution of deposits can be described by the Weibull distribution, which provides a possibility for the

quantitative study of deposition distribution. The shape parameters, which characterize the overall profile of the deposits, were influenced by the sediment concentration of the debris flow. The scale parameters, which characterize the dispersion degree of deposition, were positively correlated with the sediment filling rate, and empirical relationships among these parameters were proposed. Moreover, the topographic relief in the cross-section caused by the uneven distribution of deposition was positively correlated with the sediment filling rate and quantified with a new parameter coefficient of the topographic relief in the cross-section with a maximum value of 0.25.

#### Data availability statement (DAS)

The authors agree to make the data supporting the results or analyses presented in this paper available upon reasonable request from the first author and corresponding author.

## **CRediT authorship contribution statement**

**Jiangang Chen:** Writing – review & editing, Writing – original draft, Visualization, Validation, Supervision, Software, Resources, Project administration, Methodology, Investigation, Funding acquisition, Formal analysis, Data curation, Conceptualization. **Xi'an Wang:** Writing – original draft, Visualization, Validation, Supervision, Software, Resources, Project administration, Methodology, Investigation, Funding acquisition, Formal analysis, Data curation, Conceptualization. Huayong Chen: Writing - review & editing, Visualization, Validation, Supervision, Software, Resources, Project administration, Methodology, Investigation, Funding acquisition, Formal analysis, Data curation, Conceptualization. **Wanyu Zhao:** Writing – review & editing, Visualization, Validation, Supervision, Software, Resources, Project administration, Methodology, Investigation, Funding acquisition, Formal analysis, Data curation, Conceptualization. Chenyuan Wang: Visualization, Supervision, Investigation. Xiaoqing Chen: Writing - review & editing, Writing - original draft, Visualization, Validation, Supervision, Software, Resources, Project administration, Methodology, Investigation, Funding acquisition, Formal analysis, Data curation, Conceptualization.

# **Declaration of competing interest**

The authors declare that they have no known competing financial interests or personal relationships that could have appeared to influence the work reported in this paper.

# Acknowledgements

This study was supported by the National Natural Science Foundation of China (No. 41925030), the Second Tibetan Plateau Scientific Expedition and Research Program (No. 2019QZKK0904), and the Chinese Academy of Sciences "Light of West China" Program. Support from the Dongchuan Debris Flow Observation and Research Station (DDFORS), Chinese Academy of Sciences, is acknowledged. The authors would also like to thank the journal editors and three anonymous reviewers for their valuable suggestions.

#### References

Abbasi, N. A., Xu, X., Lucas-Borja, M. E., Dang, W., & Liu, B. (2019). The use of check dams in watershed management projects: Examples from around the world.

- Science of the Total Environment, 676, 683-691.
- Alcoverro, J., Corominas, J., & Gómez, M. (1999). The Barranco de Arás flood of 7 August 1996 (Biescas, Central Pyrenees, Spain). Engineering Geology, 51(4), 237–255.
- Armanini, A., & Larcher, M. (2001). Rational criterion for designing opening of slitcheck dam. *Journal of Hydraulic Engineering*, 127(2), 94–104.
- Bernard, M., Boreggio, M., Degetto, M., & Gregoretti, C. (2019). Model-based approach for design and performance evaluation of works controlling stony debris flows with an application to a case study at Rovina di Cancia (Venetian Dolomites, Northeast Italy). Science of the Total Environment, 688, 1373–1388.
- Campisano, A., Cutore, P., & Modica, C. (2014). Improving the evaluation of slitcheck dam trapping efficiency by using a 1D unsteady flow numerical model. *Journal of Hydraulic Engineering*, 140(7), Article 04014024.
   Castillo, V. M., Mosch, W. M., García, C. C., Barberá, G. G., Cano, J. N., & López-
- Castillo, V. M., Mosch, W. M., García, C. C., Barberá, G. G., Cano, J. N., & López-Bermúdez, F. (2007). Effectiveness and geomorphological impacts of check dams for soil erosion control in a semiarid Mediterranean catchment: El Cárcavo (Murcia, Spain). Catena, 70(3), 416–427.
- Castillo, C., Pérez, R., & Gómez, J. A. (2014). A conceptual model of check dam hydraulics for gully control: Efficiency, optimal spacing and relation with steppools. *Hydrology and Earth System Sciences*, *18*(5), 1705–1721.
- Chen, X. Q., Chen, J. G., Zhao, W. Y., Li, Y., & You, Y. (2017). Characteristics of a debrisflow drainage channel with a step-pool configuration. *Journal of Hydraulic Engineering*, 143(9), Article 04017038.
- Chen, J. G., Chen, X. Q., Zhao, W. Y., & You, Y. (2016). Discussion of 'design of sediment traps with open check dams. I: Hydraulic and deposition processes' by guillaume Piton and alain recking. *Journal of Hydraulic Engineering*, 142(10), 07016008-1.
- Chen, J. G., Chen, X. Q., Zhao, W. Y., & You, Y. (2018). Debris flow drainage channel with energy dissipation structures: Experimental study and engineering application. *Journal of Hydraulic Engineering*, 144(10), Article 06018012.
- Chen, X. Q., Cui, P., You, Y., Chen, J. G., & Li, D. J. (2015). Engineering measures for debris flow hazard mitigation in the Wenchuan earthquake area. *Engineering Geology*, 194, 73–85.
- Choi, C. E., Ng, C. W. W., Au-Yeung, S. C. H., & Goodwin, G. R. (2015). Froude characteristics of both dense granular and water flows in flume modelling. *Landslides*, *12*(6), 1197–1206.
- Church, M., & Jakob, M. (2020). What is a debris flood? *Water Resources Research*, 56(8), Article e2020WR027144.
- Cucchiaro, S., Cavalli, M., Vericat, D., Crema, S., Llena, M., Beinat, A., ... Cazorzi, F. (2019). Geomorphic effectiveness of check dams in a debris-flow catchment using multi-temporal topographic surveys. *Catena*, 174, 73–83.
- Cui, P., Zeng, C., & Lei, Y. (2015). Experimental analysis on the impact force of viscous debris flow. *Earth Surface Processes and Landforms*, 40(12), 1644–1655.
- De Haas, T., Braat, L., Leuven, J. R., Lokhorst, I. R., & Kleinhans, M. G. (2015). Effects of debris flow composition on runout, depositional mechanisms, and deposit morphology in laboratory experiments. *Journal of Geophysical Research: Earth Surface*, 120(9), 1949–1972.
- Du, J. H., Zhou, G. G., Tang, H., Turowski, J., & Cui, K. F. (2023). Classification of stream, hyperconcentrated, and debris flow using dimensional analysis and machine learning. Water Resources Research, 59(2).
- Faug, T. (2015). Macroscopic force experienced by extended objects in granular flows over a very broad Froude-number range. *The European Physical Journal E*, 38(5), 1–10.
- Gong, S., Zhao, T., Zhao, J., Dai, F., & Zhou, G. G. D. (2021). Discrete element analysis of dry granular flow impact on slit dams. *Landslides*, *18*, 1143–1152.
- Goodwin, G. R., & Choi, C. E. (2020). Slit structures: Fundamental mechanisms of mechanical trapping of granular flows. Computers and Geotechnics, 119, Article 103376.
- Hairsine, P. B., Beuselinck, L., & Sander, G. C. (2002). Sediment transport through an area of net deposition. *Water Resources Research*, 38(6), 22, 1.
- Han, W., & Ou, G. (2006). Efficiency of slit dam prevention against non-viscous debris flow. Wuhan University Journal of Natural Sciences, 11(4), 865–869.
- Huang, T., Ding, M., Gao, Z., & Téllez, R. D. (2021). Check dam storage capacity calculation based on high-resolution topogrammetry: Case study of the Cutou Gully, Wenchuan County, China. Science of the Total Environment, 790, Article 148083
- Huang, C. H., Wells, L. K., & Norton, L. D. (1999). Sediment transport capacity and erosion processes: Model concepts and reality. Earth Surface Processes and Landforms, 24(6), 503-516.
- Huebl, J., & Fiebiger, G. (2005). Debris-flow mitigation measures. In *Debris-flow hazards and related phenomena* (pp. 445–497). Berlin, Heidelberg: Springer Praxis Books.
- Ishikawa, N., Fukawa, G., Katsuki, S., & Yamada, G. (2004). Catch effect of debris flow for the open type steel check dam by physical and numerical modeling. In Proc., INTERPRAEVENT conf., 3 (pp. 153–163). Klagenfurt, Austria: International Research Society INTERPRAEVENT.
- Ishikawa, N., Shima, J., Matsubara, T., Tatesawa, H., Horiguchi, T., & Mizuyama, T. (2014). Trapping mechanism of debris flow by steel open dams. Proc. INTER-PRAEVENT International Symposium, Nara, Japan, 185–190.
- James, M. R., & Robson, S. (2012). Straightforward reconstruction of 3D surfaces and topography with a camera: Accuracy and geoscience application. *Journal of Geophysical Research: Earth Surface*, 117, Article F03017, 17.
- Kaitna, R., & Huebl, J. (2013). Silent witnesses for torrential processes. In M. Schneuwly-Bollschweiler, M. Stoffel, & F. Rudolf-Miklau (Eds.), Advances in global change research: 47. Dating torrential processes on fans and cones (pp.

- 111-130). Dordrecht: Springer.
- Li, S., You, Y., Chen, X., Liu, J., & Chen, J. (2019). Regulation effectiveness of a window-check dam on debris flows. *Engineering Geology*, 253, 205–213.
- Li, X., Zhao, J., & Soga, K. (2021). A new physically based impact model for debris flow. Géotechnique, 71(8), 674–685.
- Lien, H. P. (2003). Design of slit dams for controlling stony debris flows. *International Journal of Sediment Research*, 18(1), 74–87.
- Liu, J., Nakatani, K., & Mizuyama, T. (2013). Effect assessment of debris flow mitigation works based on numerical simulation by using Kanako 2D. *Landslides*, 10(2), 161–173.
- Liu, W., Yan, S., & He, S. (2020). A simple method to evaluate the performance of an intercept dam for debris-flow mitigation. *Engineering Geology*, 276, Article 105771.
- Lucas-Borja, M. E., Piton, G., Yu, Y., Castillo, C., & Zema, D. A. (2021). Check dams worldwide: Objectives, functions, effectiveness and undesired effects. *Catena*, 204. Article 105390.
- Lucas-Borja, M. E., Zema, D. A., Guzman, M. D. H., Yang, Y., Hernández, A. C., Xiangzhou, X., ... Cerdá, A. (2018). Exploring the influence of vegetation cover, sediment storage capacity and channel dimensions on stone check dam conditions and effectiveness in a large regulated river in México. Ecological Engineering, 122, 39–47.
- Major, J. J., & Iverson, R. M. (1999). Debris-flow deposition: Effects of pore-fluid pressure and friction concentrated at flow margins. Geological Society of America Bulletin, 111(10), 1424–1434.
- Marchelli, M., Leonardi, A., Pirulli, M., & Scavia, C. (2020). On the efficiency of slitcheck dams in retaining granular flows, *Géotechnique*, 70(3), 226–237.
- Mergili, M., Pudasaini, S. P., Emmer, A., Fischer, J. T., Cochachin, A., & Frey, H. (2020).

  Reconstruction of the 1941 GLOF process chain at lake palcacocha (Cordillera Blanca. Peru). Hydrology and Earth System Sciences. 24(1), 93–114.
- Blanca, Peru). *Hydrology and Earth System Sciences*, 24(1), 93–114.

  Ng, C. W. W., Choi, C. E., & Goodwin, G. R. (2019). Froude characterization for unsteady single-surge dry granular flows: Impact pressure and runup height. *Canadian Geotechnical Journal*, 56(12), 1968–1978.
- Osti, R., & Egashira, S. (2013). Sediment transportation from bed-load to debris-flow and its control by check dams in torrential streams. In C. Conesa-Garcia, & M. A. Lenzi (Eds.), *Check dams, morphological adjustments and erosion control in torrential streams* (pp. 151–184). New York: Nova Science Publishers, Inc.
- Piton, G., Carladous, S., Recking, A., Tacnet, J. M., Liébault, F., Kuss, D., ... Marco, O. (2017). Why do we build check dams in alpine streams? An historical perspective from the French experience. Earth Surface Processes and Landforms, 42(1), 91–108.
- Piton, G., & Recking, A. (2016a). Design of sediment traps with open check dams. I: Hydraulic and deposition processes. *Journal of Hydraulic Engineering*, 142(2), Article 04015045.
- Piton, G., & Recking, A. (2016b). Design of sediment traps with open check dams. Il: Woody debris. *Journal of Hydraulic Engineering*, 142(2), Article 04015046.
- Pudasaini, S. P., & Krautblatter, M. (2021). The mechanics of landslide mobility with erosion. *Nature Communications*, 12, 6793.
- Qin, C., Zheng, F., Wells, R. R., Xu, X., Wang, B., & Zhong, K. (2018). A laboratory study of channel sidewall expansion in upland concentrated flows. *Soil and Tillage Research*, 178, 22–31.
- Ran, Q., Tang, H., Wang, F., & Gao, J. (2021). Numerical modelling shows an old check-dam still attenuates flooding and sediment transport. *Earth Surface Pro*cesses and Landforms, 46(8), 1549–1567.
- Rickenmann, D. (1999). Empirical relationships for debris flows. *Natural Hazards*,
- Robichaud, P. R., Storrar, K. A., & Wagenbrenner, J. W. (2019). Effectiveness of straw bale check dams at reducing post-fire sediment yields from steep ephemeral

- channels. Science of the Total Environment, 676, 721-731.
- Schwindt, S., Franca, M. J., De Cesare, G., & Schleiss, A. J. (2017). Analysis of mechanical-hydraulic bedload deposition control measures. *Geomorphology*, 295, 467–479.
- Schwindt, S., Franca, M. J., Reffo, A., & Schleiss, A. J. (2018). Sediment traps with guiding channel and hybrid check dams improve controlled sediment retention. *Natural Hazards and Earth System Sciences*, *18*(2), 647–668.
- Shima, J., Moriyama, H., Kokuryo, H., Ishikawa, N., & Mizuyama, T. (2016). Prevention and mitigation of debris flow hazards by using steel open-type Sabo dams. *International Journal of Erosion Control Engineering*, 9(3), 135–144.
- Shrestha, B. B., Nakagawa, H., Kawaike, K., & Baba, Y. (2008). Numerical simulation on debris-flow deposition and erosion processes upstream of a check dam with experimental verification, 51 (pp. 613–624). Annual Disaster Prevention Research Insitute, Kyoto University.
- Silva, M., Costa, S., Canelas, R. B., Pinheiro, A. N., & Cardoso, A. H. (2016). Experimental and numerical study of slit-check dams. *International Journal of Sustainable Development and Planning*, 11(2), 107–118.
- Song, D., Chen, X., Zhou, G. G., Lu, X., Cheng, G., & Chen, Q. (2021). Impact dynamics of debris flow against rigid obstacle in laboratory experiments. *Engineering Geology*, 291, Article 106211.
- Sun, H., You, Y., & Liu, J. (2018). Experimental study on blocking and self-cleaning behaviors of beam dam in debris flow hazard mitigation. *International Journal of Sediment Research*, 33(4), 395–405.
- Takahashi, T. (2009). A review of Japanese debris flow research. *International Journal of Erosion Control Engineering*, *2*(1), 1–14.

  Takahiro, I. T. O. H., Horiuchi, S., Mizuyama, T., & Kaitsuka, K. (2013). Hydraulic
- Takahiro, I. T. O. H., Horiuchi, S., Mizuyama, T., & Kaitsuka, K. (2013). Hydraulic model tests for evaluating sediment control function with a grid-type Sabo dam in mountainous torrents. *International Journal of Sediment Research*, 28(4), 511–522.
- Vaezi, A. R., Abbasi, M., Keesstra, S., & Cerdà, A. (2017). Assessment of soil particle erodibility and sediment trapping using check dams in small semi-arid catchments. Catena. 157, 227–240.
- Van Oost, K., Beuselinck, L., Hairsine, P. B., & Govers, G. (2004). Spatial evaluation of a multi-class sediment transport and deposition model. *Earth Surface Processes and Landforms*, 29(8), 1027–1044.
- Wang, X. A., Chen, J. G., Chen, H. Y., Chen, X. Q., Li, S., & Zhao, W. Y. (2022). Erosion process of multiple debris flow surges caused by check dam removal: An experimental study. *Water Resources Research*, 58(3), Article e2021WR030688.
- Wang, F., Wang, J., Chen, X., & Chen, J. (2019). The influence of temporal and spatial variations on phase separation in debris flow deposition. *Landslides*, *16*(3), 497–514.
- Wang, X. A., Chen, J. G., Chen, X. Q., Chen, H. Y., Zhao, W. Y., Ruan, H. C., & Wang, J. S. (2024). Bank retreat mechanisms driven by debrisflow surges: A parameterized model basedon the results of physical experiments. Water Resources Research, 60. e2023WR036914.
- Wu, J. S., Tian, L. Q., Kang, Z. C., Zhang, Y. F., & Liu, J. (1993). Debris flow and its comprehensive control. Beijing: Science Press (in Chinese).
- You, Y., Lin, X. P., Liu, J. F., & Zhao, Y. B. (2013). One calculation method of deposition shape behind the debris-flow check dam and its application. In *Authorization announcement No. CN* 103276687. Copernicus GmbH (in Chinese).
- Zhou, G. G. D., Hu, H. S., Song, D., Zhao, T., & Chen, X. Q. (2019a). Experimental study on the regulation function of slit dam against debris flows. *Landslides*, 16(1), 75–90.
- Zhou, G. G. D., Li, S., Song, D., Choi, C. E., & Chen, X. (2019b). Depositional mechanisms and morphology of debris flow: Physical modelling. *Landslides*, 16(2), 315–332.